

Quantum to classical transition in a system with a mixed classical dynamics

Fabrizio Toscano

*Fundação Centro de Ciências e Educação Superior à Distância do
Estado do Rio de Janeiro, 20943-001 Rio de Janeiro, RJ, Brazil. and
Instituto de Física, Universidade Federal do Rio de Janeiro, Cx. P. 68528,
21941-972 Rio de Janeiro, RJ, Brazil.*

Diego A. Wisniacki

*Departamento de Física "J. J. Giambiagi", FCEN, UBA, 1428 Buenos Aires, Argentina.
(Dated: November 14, 2021)*

We study how decoherence rules the quantum-classical transition of the Kicked Harmonic Oscillator (KHO). When the amplitude of the kick is changed the system presents a classical dynamics that range from regular to a strong chaotic behavior. We show that for regular and mixed classical dynamics, and in the presence of noise, the distance between the classical and the quantum phase space distributions is proportional to a single parameter $\chi \equiv K\hbar_{\text{eff}}^2/4D^{3/2}$ which relates the effective Planck constant \hbar_{eff} , the kick amplitude K and the diffusion constant D . This is valid when $\chi < 1$, a case that is always attainable in the semiclassical regime independently of the value of the strength of noise given by D . Our results extend a recent study performed in the chaotic regime.

PACS numbers: 05.45.-a, 03.65.Ta

I. INTRODUCTION

The complete description of the emergence of the classical world within the quantum theory is a fundamental problem that have attracted a lot of attention since the beginning of quantum mechanics. Although many advances have been made, there are still open questions. An important step forward was done with the understanding that the formalism of phase space distribution functions is the appropriate framework to study the quantum to classical transition [1]. Among all quantum phase-space distributions, the Wigner function [2] has the advantage that identifies the nonlinearities of the system as the responsible for the separation between the quantum and the classical evolution. Indeed, while for linear systems the Wigner distribution obey the Liouville equation of the classical distribution, the nonlinearities add terms to this equation that eventually set the two distributions apart [3], even for initial states that are classically allowed.

The time for which classical and quantum distributions starts to differ, called breaking or separation time, can be very short for classically chaotic systems. This is because the nonlinearities of the system are reached very quickly due to the exponential stretching of the distributions. Hence, the breaking time scale as $\ln(1/\hbar_{\text{eff}})$, where the effective Planck constant $\hbar_{\text{eff}} \equiv \hbar/S$ is the semiclassical parameter (with S a typical action of the system) [4, 5, 6, 7, 8, 9, 10].

An important and subtle problem is that the breaking time for macroscopic systems ($\hbar_{\text{eff}} \ll 1$) can still be small compared to a typical evolution time due to its logarithmic behavior, allowing quantum effects that are not observed in the classical world [11]. This paradoxical situation is explained by the coupling of the system with the environment, which leads to the elimination of

the quantum signatures, providing the reconciliation of theory and observation [12, 13]. At this respect, an open question is how the effects of the environment affect the logarithmic law of the breaking time in systems with a classical chaotic dynamics. More precisely, we can say that it is still unknown the exact relation between the strength of noise and the effective Planck constant in order to obtain the correct classical limit [14].

This problem has started to be answer in a recent work [15] where the authors study the effect of a purely diffusive environment over an specific model given by the Kicked Harmonic Oscillator (KHO). They show that the differences between the classical and quantum phase evolution is proportional to a single parameter $\chi = K\hbar_{\text{eff}}^2/4D^{3/2}$, that combine \hbar_{eff} , the diffusion coefficient D and the kicking strength K , who control the macroscopicity, the noise and the chaotic behavior respectively. These quantum-classical differences were estimated with \mathcal{D}_n (n is the number of kicks) which is the integral over the whole phase space of the modulus of the difference between the quantum and the classical distributions. Thus, it was shown that, when the classical dynamics is chaotic, in the semiclassical limit $\hbar_{\text{eff}} \ll 1$ and when $\chi < 1$, the single parameter χ controls the quantum-classical transition of the KHO. This result, confirm the conjecture presented in Ref. [16] that in the presence of noise a single parameter controls the quantum-classical transition of classically chaotic systems.

In this paper we analyze the case when the classical dynamics of the KHO is regular or mixed. In the absence of a reservoir, we show that the separation between the quantum and the classical evolution can be characterized through the behavior of \mathcal{D}_n as a function of time. When the initial distribution explore regions of regular classical dynamics, the behavior of \mathcal{D}_n allows the identification of a potential scale-law $1/\hbar_{\text{eff}}^\alpha$ for the separation time.

However, this scale-law is not valid when the degree of mixing increase. In the presence of a purely diffusive reservoir, we show that the quantum-classical differences measured by \mathcal{D}_n , still scale with the parameter χ in the semiclassical limit and when $\chi < 1$. Hence, the concept of separation time is not meaningful anymore, since the quantum and the classical distributions remain close throughout the evolution. Our result suggest that the conjecture in [16] can be extended independently of the underlying classical dynamics.

The paper is organized as follows. Section II is devoted to review the quantum and the classical versions of the KHO and also to explain the formalism for the evolution of the Wigner function and the classical distribution as a map in phase space. In Section III we introduce our measure of the quantum-classical differences \mathcal{D}_n , and study its behavior as a function of time without the presence of a reservoir. We investigate the scale-law with the effective Planck constant of the separation time when the initial distribution explore regular or mixed regions of the phase space. The effects of decoherence over \mathcal{D}_n , when the KHO is in contact with a purely diffusive reservoir, is studied in Section IV. We end with some final remarks in Section V.

II. MODEL: THE KICKED HARMONIC OSCILLATOR

A. The quantum version

The model used in our calculations is the KHO, a particle of mass m in a harmonic potential subjected to a periodically applied position-dependent delta pulses. The quantum Hamiltonian is defined as:

$$\hat{H} = \frac{\hat{P}^2}{2m} + \frac{1}{2}m\nu^2\hat{Q}^2 + A \cos(k\hat{Q}) \sum_{n=0}^{\infty} \delta(t - n\tau), \quad (1)$$

where ν is the oscillator frequency, A the amplitude of the kicks and τ the interval between two consecutive kicks. k sets the periodicity of the position dependent kicking potential. The physical realization of this Hamiltonian is within the context of trapped ions. It was shown in Ref. [17], that it describes the center-of-mass dynamics of an ion in a one-dimensional trap submitted to a sequence of standing-wave laser-pulses, off-resonance with a transition between the electronic ground state and another internal state. The wave number k in Eq. (1) is the projection along the trap axis of the corresponding wave vectors with equal modulus $|\vec{k}|$ of two opposite propagating pulses with oblique incidence measured by an angle θ , *i.e.* $k \equiv 2|\vec{k}|\cos(\theta)$.

It is possible to define an effective Planck constant \hbar_{eff} if we work with dimensionless quantities $\hat{q} = k\hat{Q}$, $\hat{p} = k\hat{P}/m\nu$, and $K = k^2 A/m\nu$, so that $[\hat{q}, \hat{p}] = 2i\eta^2 \equiv i\hbar_{\text{eff}}$, with $\eta = k\Delta Q_0 = k\sqrt{\hbar/2m\nu}$, and ΔQ_0 being the width of the ground state of the harmonic oscillator. The

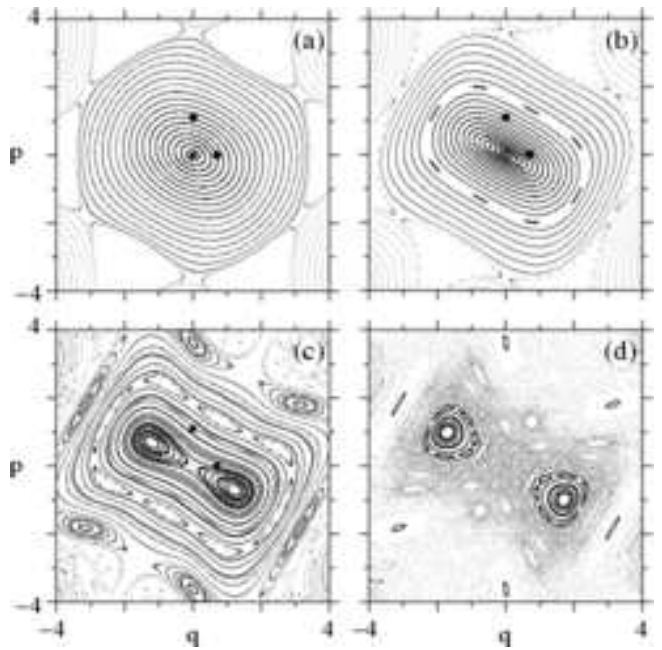


FIG. 1: Stroboscopic phase space of the KHO for different values of the kicked amplitude K . In (a) $K = 0.5$, (b) $K = 1.0$, (c) $K = 1.5$ and in (d) $K = 2.0$. The phase space points $(q_0, p_0) = (0, 0)$, $(0, 1.1)$ and $(0.7, 0)$, marked with symbols (•), are the centers of the initial coherent states used in our numerical simulations.

dimensionless parameter η is the so-called Lamb-Dicke parameter [18], which measures the ratio between the ground state width and the wavelength $\lambda = 2\pi/k$ that sets the scale of the non-linearity of the Hamiltonian. In experiments with trapped ions, the classical limit $\eta \rightarrow 0$ (and thus $\hbar_{\text{eff}} \equiv 2\eta^2 \rightarrow 0$) can be approximated simply by changing the angle θ of incidence of the incoming pulses, or by increasing the trap frequency ν .

B. The classical dynamics.

The classical Hamiltonian is obtained from Eq.(1) simply by replacing the quantum operators \hat{Q} and \hat{P} by the phase space variables Q and P respectively. In an analogous way we can define the dimensionless phase space coordinates $\mathbf{x} \equiv (q, p) \equiv (kQ, kP/m\nu)$. Then, the time-dependent classical evolution can be described as a composition of a discrete map corresponding to the kick, plus a rotation in phase space: $\mathbf{x}_{n+1} = \mathbf{R} \circ \mathbf{K}(\mathbf{x}_n)$ where $\mathbf{x}_n \equiv (q_n, p_n)$ are the coordinates before kick n (where the first kick corresponds to $n = 0$). The kick operation \mathbf{K} is defined as

$$q_n^+ = q_n, \quad p_n^+ = p_n + K \sin(q_n), \quad (2)$$

and the phase space rotation \mathbf{R} is given by:

$$\begin{aligned} q_{n+1} &= \cos(\nu\tau) q_n^+ + \sin(\nu\tau) p_n^+, \\ p_{n+1} &= -\sin(\nu\tau) q_n^+ + \cos(\nu\tau) p_n^+. \end{aligned} \quad (3)$$

In close relation with Ref. [15], we also consider the case where the interval between kicks τ and the period of the harmonic oscillator $T = 2\pi/\nu$ are related by $\tau = T/6$.

The phase space of the system is unbounded and corresponds to a mixed dynamics exhibiting stable islands surrounded by a stochastic web along which the particle diffuses. The thickness of the web is controlled by the chaoticity parameter $K = k^2 A/m\nu$ which is the dimensionless kicked amplitude. Hence, these chaotic regions broadens (shrinks) as K increases (decreases). In the case of $\tau = T/6$ considered, the stochastic web displays crystal hexagonal symmetry [7, 9]. In Fig.1 we show the stroboscopic phase space around the origin for different values of K . For $K \leq K_c \approx 1.1547$ the origin is an elliptic fixed point while for $K > K_c$ the system undergoes a bifurcation where the origin become an hyperbolic fixed point and two neighbor elliptic fixed points arise. The separation between these two elliptic fixed points increases with K . As we can see in Fig.1(a), for $K = 0.5$ the dynamics of the system around the origin is essentially regular with a series of concentric tori around the elliptic fixed point. For $K = 1$ [Fig 1(b)], some tori were destroyed, and tiny chaotic regions appear (invisible to the eye). Mixed dynamics start to manifest most appreciable for $K = 1.5$ while for $K = 2$ most of the area around the origin shows chaotic behavior [see Fig .1(c) and (d)].

C. The evolution of phase space distributions without reservoir.

We analyze the quantum-classical transition in phase space comparing the evolution of the Wigner function [2] and the corresponding classical distribution. The Wigner function, defined as

$$W(\mathbf{x}) \equiv \int dy \left\langle q + y/2 \left| \frac{\hat{\rho}}{4\pi\eta^2} \right| q - y/2 \right\rangle \exp \left\{ -i \frac{py}{2\eta^2} \right\}, \quad (4)$$

with $\hat{\rho}$ the density operator of the quantum state, have a highlight position within all the quantum quasiprobability distribution in phase space because it is the only one to yield the correct marginal probabilities, thus satisfying an important property of classical distributions [19]. Furthermore, quantum effects are more pronounced, as compared to other bounded distributions. Finally, new methods have been developed for the direct measurement of the Wigner function, which are adequate for the description of evolving systems [20].

Without the action of a reservoir the unitary evolution of the Wigner function of the KHO can be written as

[5, 15]

$$W_{n+1}(\mathbf{x}) = \int d\mathbf{x}' L(\mathbf{x}^R, \mathbf{x}') W_n(\mathbf{x}'), \quad (5)$$

where W_{n+1} and W_n are the Wigner functions immediately before the kicks $n+1$ and n respectively. The integration is over all the unbounded phase space, and

$$\begin{aligned} L(\mathbf{x}^R, \mathbf{x}') &\equiv \int_{-\infty}^{\infty} \frac{d\mu}{2\pi\eta^2} e^{\frac{i}{\eta^2} [K \sin(q') \sin(\mu) - \mu(p^R - p')] } \times \\ &\times \delta(q^R - q'), \end{aligned} \quad (6)$$

is the quantum propagator of one kick plus the harmonic evolution between the consecutive kicks which is given by

$$\mathbf{x}^R \equiv [q^R(\mathbf{x}), p^R(\mathbf{x})] \equiv \mathbf{R}^{-1}(\mathbf{x}), \quad (7)$$

i.e. the phase space coordinates rotated with the inverse transformation of Eq. (3). The Liouville evolution of the classical distribution $W_n^{cl}(\mathbf{x})$ can also be written in the form of Eq. (5) with the classical propagator

$$L^{cl}(\mathbf{x}^R, \mathbf{x}') \equiv \delta[p' - p^R + K \sin(q')] \delta(q^R - q'). \quad (8)$$

In the classical limit $\eta \rightarrow 0$ the classical propagator is formally recovered from the quantum one [5]. Indeed, in the semiclassical regime ($\eta \ll 1$) the integral in Eq.(6) can be estimated employing stationary-phase techniques yielding,

$$\begin{aligned} L(\mathbf{x}^R, \mathbf{x}') &\approx \frac{1}{|b|^{1/3}} \text{Ai} \left(-\frac{\text{sign}(b)}{|b|^{1/3}} (p' - p^R + K \sin(q')) \right) \times \\ &\times \delta(q^R - q'), \end{aligned} \quad (9)$$

where $b = (\eta^4 K/2) \sin(q')$ and $\text{Ai}(x)$ is the Airy function. When $\eta \rightarrow 0$ we can use that $\text{Ai}\{-y/\varepsilon\}/\varepsilon \xrightarrow{\varepsilon \rightarrow 0} \delta(y)$ to get the classical Liouville propagator in Eq.(8). However, no matter how small we can do the Lamb-Dicke parameter η in a physical realization of the KHO, this will always take a finite value and then the presence of an Airy function in the quantum propagator will eventually set the Wigner function and the classical distribution apart.

III. THE QUANTUM-CLASSICAL SEPARATION WITHOUT RESERVOIR: SCALE-LAW FOR THE SEPARATION TIME.

The Wigner distribution of a linear system (quadratic Hamiltonian) satisfy the Liouville equation for the classical phase-space probability distribution. Thus, if we start with a Wigner function of a classically allowed probability distribution (the only possibility is a minimum uncertainty initial Gaussian wave packet [22]), the linear dynamics evolution will preserve its Gaussian shape. When the system have non-linearities, the initial wave packet will deform and eventually delocalized during the

evolution. As a consequence, quantum interference effects appear between different pieces of the wave packet, which remains coherent throughout the unitary evolution. These quantum interference effects stem from the extra terms that the non-linearities of the system add to the Liouville equation in order to obtain the correct equation of motion of the Wigner function [3, 23]. Equivalently, we can say that these interferences are originated by the non-local nature of the Wigner propagator (see for example Eq.(6)) in comparison with the local nature of the Liouville propagator of Eq.(8), that persist even in the semiclassical regime [see Eq.(9)]. Hence, they are the responsible for the separation of the Wigner function from the classical distribution and thus of the quantum-classical correspondence breakdown.

The quantum-classical differences start to become important when the initial distribution spreads over distances of the order of the characteristic scale of the nonlinearities of the system, and it is well known this argumentation in order to estimate the time scale for the separation in the case of classically chaotic systems [11, 13, 24]. Indeed, as the initial Gaussian Wigner function is well localized, it will initially evolve following classical trajectories in phase space, therefore the wave packet will stretch exponentially fast along the unstable manifold and will shrink also exponentially fast along the stable one in order to conserve the phase space volume. This is also accompanied by the characteristic folding of classical trajectories that forces the wave packet to develop quantum interference between different pieces which are coherently related. As a result of this behavior, it is found a logarithmic scale law with the effective Planck constant \hbar_{eff} of the separation time in systems with classical chaotic dynamics. For the KHO, the estimation of the separation time t_s gives

$$t_s = n_s \tau \approx \frac{\tau}{\Lambda} \ln(1/\eta) \quad (10)$$

where Λ is the local expansion coefficient and $\hbar_{\text{eff}} = 2\eta^2$. A detailed estimation of t_s can be found in Ref. [7, 10] and in [9], where it is also shown a numerical test that indicates that this is also the time when quantum and classical expectation values start to differ from each other. The expansion coefficient Λ corresponds to the Lyapunov exponent when an average over initial conditions in the chaotic regions is considered [10, 15].

In the other extreme situation, when the classical dynamics of the system is essentially regular, the scaling law of the quantum-classical separation time with \hbar_{eff} was less studied. The logarithmic dependence of t_s in the chaotic case is due to the exponential divergence of classical trajectories, but in the integrable case the divergence is typically polynomial [13, 25]. Therefore, following a similar type of argumentation that in the chaotic case, the separation time in regular systems would follow a potential scale-law with \hbar_{eff} . In the case of the KHO, if the initial distribution explores regions of essentially

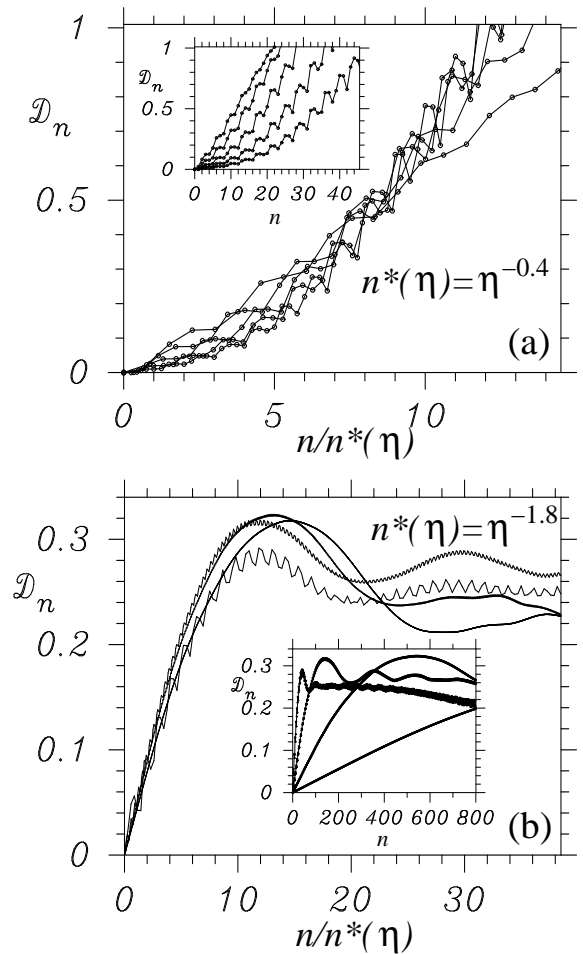


FIG. 2: Separation D_n between quantum and classical distribution as a function of the number of kicks for $K = 0.5$. The full lines joint all the values of D_n calculated for the same value of the Lamb-Dicke parameter η . In (a) the initial distribution is a coherent state centered at the phase space point $(q_0, p_0) = (0, 1.1)$ and the curves are for the decreasing values of $\eta = 0.5, 0.25, 0.125, 0.0625$ and 0.03125 . The result for the initial condition $(q_0, p_0) = (0.7, 0)$ is equivalent (not plotted here). In (b) the initial coherent state is centered at the origin and the curves are for $\eta = 0.5, 0.25, 0.125$ and 0.0625 . The number of kicks n are rescaled by a function $n^*(\eta) = \eta^{-\alpha}$ where we optimize the values of α in order to obtain the best collapsing of all the curves. The insets show the curves without the rescaling over the time n .

regular dynamics, we would have

$$t_s = n_s \tau \approx \tau / \eta^\alpha, \quad (11)$$

where numerical constants are forbidden. Indications of the validity of Eq.(11) for $K \ll 1$ are given in Ref. [7]. In what follows we show a way to estimate the amount of quantum effects that lead to the separation between the Wigner function and the classical distribution, and how the scaling law for the separation time in Eq.(11) manifests in our formalism.

In Ref. [15], it was introduced the time dependent

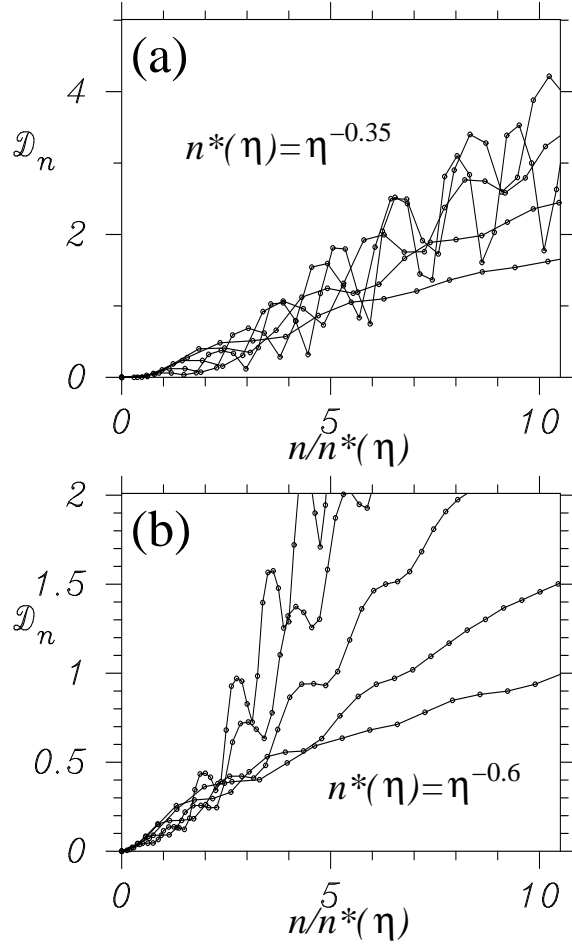


FIG. 3: Idem as Fig.2 but for $K = 1.0$. In **a**) the initial coherent state centered at $(q_0, p_0) = (0, 1.1)$ and in **b**) $(q_0, p_0) = (0.7, 0)$. The different curves in each plot corresponds to $\eta = 0.5, 0.25, 0.125, 0.0625$ and 0.03125 . The number of kicks n are rescaled by a function $n^*(\eta) = \eta^{-\alpha}$ where we optimize the values of α in order to obtain the best collapsing of all the curves.

quantity ($t = n\tau$),

$$\mathcal{D}_n \equiv \int d\mathbf{x} |W_n(\mathbf{x}) - W_n^{cl}(\mathbf{x})|, \quad (12)$$

to quantify the quantum effects that lead to the separation between the Wigner function and the classical distribution. Here, W_n and W_n^{cl} are respectively the Wigner function and the classical distribution immediately before the kick n , both normalized to the unity. Starting with the same initial distribution it is expected that during the unitary evolution the appearance of quantum-classical differences make \mathcal{D}_n to grow and eventually saturate around some finite value. This behavior is shown in Fig.2 and 3 where we have plotted \mathcal{D}_n as a function of the scaled number of kicks (see below) for different values of the semiclassical parameter η and the amplitude of the kick K . The initial distribution is always a coherent state with width $\Delta q(0) = \Delta p(0) = \eta$.

In Fig.2 the amplitude of the kick is $K = 0.5$, so we study the case with regular classical dynamics as the different initial coherent states considered, during the interval of times monitored, spread over the regular region around the origin (see Fig. 1, 4 and 5). We can see in Fig. 2 (a) that when we start with an initial wave packet outside the origin, the quantity \mathcal{D}_n grows up to values larger than one, for all values of the semiclassical parameter η [26]. This clearly indicates the separation between the Wigner and the classical distributions because a measure of their differences reach values of the order of their normalization. However, it is important to note that no matter which value of the quantum differences, measured by \mathcal{D}_n , we choose in the plot of Fig. 2 (a) to define the separation between the Wigner and classical distributions: it will be reached at some early time of the evolution independently of how small is the semiclassical parameter η . Thus, the separation time defined in this way should scale as in Eq.(11). This is showed in the plots by the rescaling of the number of kicks by a function of the form $n^*(\eta) = \eta^{-\alpha}$ that allows the approximately collapse of all the curves. In Fig. 3 it is shown the case when the kicking amplitude is $K = 1$. We can see a similar behavior although the collapsing of all the curves do not work so well. This is an indication of the departure of the separation time from the scale-law in Eq.(11) when the degree of mixing in the classical dynamics grows. It is important to note that such scaling was not observed for the case when the kicking amplitude is $K = 1.5$.

In Fig. 2 (b) we show the case when the initial coherent state is centered at the origin of phase space when $K = 0.5$. \mathcal{D}_n grows up to values around 0.25 and then saturate for all semiclassical parameters η . In this case, \mathcal{D}_n grow less than when the initial coherent state is outside the origin because now the quantum and classical distributions remains well localized for very long times and thus the quantum-classical differences are less pronounced (Fig. 5). Nevertheless, this differences do not decrease for small values of η , showing that the separation between the classical and the quantum evolution occurs in the semiclassical regime. The fluctuations observed in Fig. 2 (a) and (b) have a period of $n \approx 6$ kicks *i.e.* approximately the period of the harmonic evolution $T = 6\tau$. This is the time that most parts of the quantum and classical distribution take to complete a spin along the elliptical structure of phase space around the origin for $K = 0.5$ (see Fig. 1).

It is interested to compare in Fig. 4 and Fig. 5 the quantum-classical differences that leads to the separation between the quantum and the classical evolution when the amplitude of the kick is $K = 0.5$. Indeed, when the initial coherent state is centered outside the origin, the quantum and classical distributions spread out and as a consequence the Wigner function develops a quantum interference pattern throughout the evolution that clearly indicates its separation from the classical distribution (see Fig. 4). Now, when the initial coherent state is centered at the origin of phase space, which is an el-

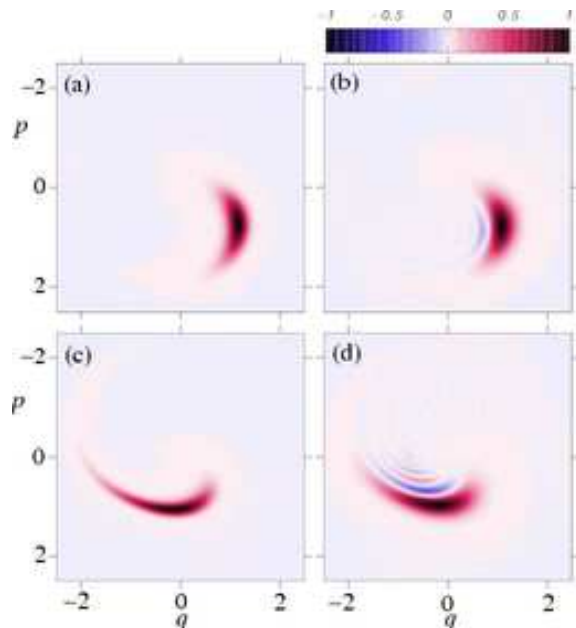


FIG. 4: Density plots of the Wigner (right) and classical distributions (left) that result from the evolution with the KHO Hamiltonian with the kick amplitude $K = 0.5$ from an initial coherent state centered in the phase space point $(q_0, p_0) = (0.0, 1.1)$ and with a width $\Delta q(0) = \Delta p(0) = \eta = 0.25$. In (a) and (b) immediately before the kick $n = 8$ and in (c) and (d) immediately before the kick $n = 18$.

liptical fixed point for $K = 0.5$, the quantum and the classical distributions remain well localized for very long times (Fig. 5). In this case, the classical distribution develops the typical classical structure of “whorls” associated with an elliptic fixed point [5, 21]. It is evident from the figure that the quantum evolution smooths out this details of the classical distribution and this is the origin of the quantum-classical differences that leads to the separation.

IV. DECOHERENCE: THE EFFECT OF A DIFFUSIVE ENVIRONMENT

Here, we study how the decoherence affects the quantum-classical differences given by the quantity \mathcal{D}_n , when the initial distribution explore phase space regions of regular or mixed classical dynamics. Our approach is in line with the one developed in Ref. [15], where the case of chaotic dynamics was studied. Therefore, we also coupled the KHO to a thermal reservoir with average population \bar{n} , in the Markovian and weak coupling limit, and we consider the purely diffusive regime [15], *i.e.* the high temperature regime $\bar{n} \rightarrow \infty$ together with $\Gamma \rightarrow 0$ but when $\bar{n}\Gamma$ is constant (Γ is the dissipation rate). In this limit, the action of the reservoir over the Wigner

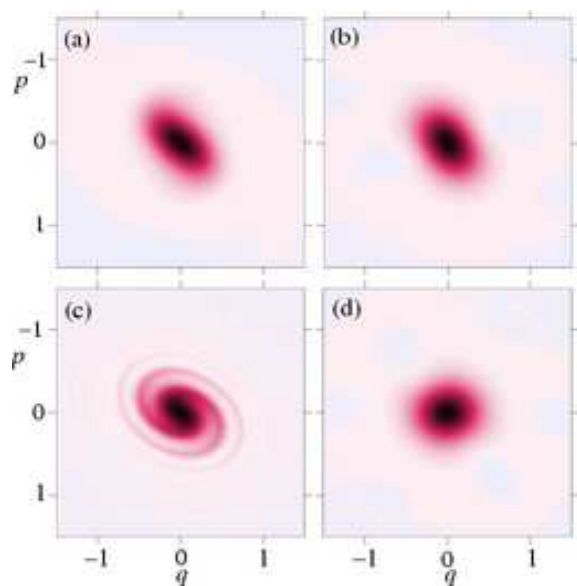


FIG. 5: Density plots of the Wigner (right) and classical distributions (left) that result from the evolution with the KHO Hamiltonian with the kick amplitude $K = 0.5$ from an initial coherent state centered at the origin of phase space and with a width $\Delta q(0) = \Delta p(0) = \eta = 0.25$. In (a) and (b) immediately before the kick $n = 60$ and in (c) and (d) immediately before the kick $n = 300$.

function is described by the Fokker-Planck equation

$$\left. \frac{\partial W}{\partial t} \right|_{\text{reservoir}} = \tilde{\Gamma} \left(\frac{\partial^2 W}{\partial q^2} + \frac{\partial^2 W}{\partial p^2} \right), \quad (13)$$

with $\tilde{\Gamma} \equiv \bar{n}\Gamma\eta^2$. For the complete evolution we have to add to right-hand side (RHS) of Eq.(13) the unitary evolution given by the Hamiltonian in Eq.(1). The action of a pure diffusive reservoir over a classical distribution is also described by Eq.(13) if we identified $\tilde{\Gamma}$ with the classical diffusion constant. In this case, we must add to the RHS of Eq.(13) the corresponding Liouville term of the classical dynamics to obtain the complete evolution.

Our findings about the behavior of the quantity \mathcal{D}_n in the presence of decoherence are a consequence of the effects of the reservoir over the one kick propagator of the Wigner function, that bring it close to the classical propagator of one kick. Hence, we first summarize the steps in Ref. [15] that allows to write the one kick propagator of the Wigner function as a function of the one kick propagator of the classical distribution under the action of a purely diffusive reservoir and in the semiclassical regime ($\eta \ll 1$).

The solution of the differential equations for the evolutions of both, the classical and the quantum distributions, in the interval of time between two consecutive kicks, and in the presence of the purely diffusive reservoir, can be written as in Eq.(5) where we have to replace the one kick propagator $L(\bar{\mathbf{x}}, \mathbf{x}')$ of Eq.(6) or (8) by the

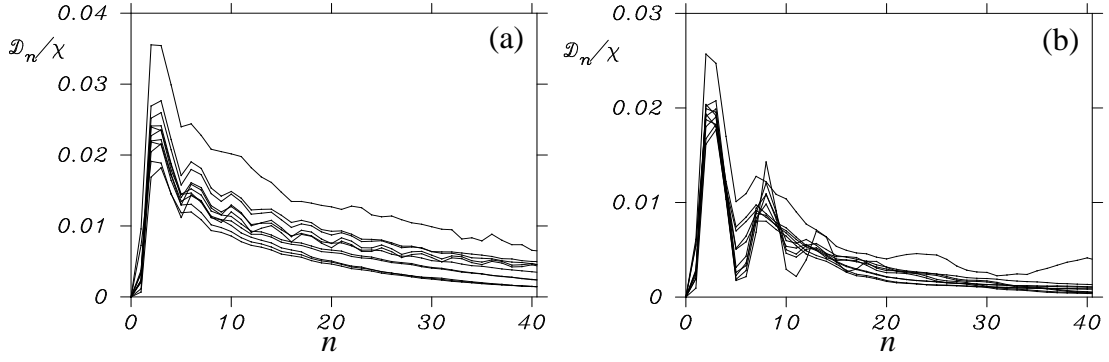


FIG. 6: Renormalized distances between quantum and classical distributions, with diffusion. All the curves were generated with the initial coherent state centered in the phase-space point $(q_0, p_0) = (0, 1.1)$ (see Fig. 1) with the kicked amplitude $K = 0.5$ in (a) and $K = 1.5$ in (b). The eleven different curves correspond to $\chi \equiv K\eta^4/D^{3/2} = 6.2 \times 10^{-2}, 4.3 \times 10^{-2}, 1.5 \times 10^{-2}, 1.1 \times 10^{-2}, 7.6 \times 10^{-3}, 3.9 \times 10^{-3}, 1.4 \times 10^{-3}, 6.8 \times 10^{-4}, 4.8 \times 10^{-4}, 2.4 \times 10^{-4}, 4.3 \times 10^{-5}$ in (a) and $\chi = 6.5 \times 10^{-2}, 4.5 \times 10^{-2}, 3.3 \times 10^{-2}, 2.3 \times 10^{-2}, 1.2 \times 10^{-2}, 4.1 \times 10^{-3}, 2.1 \times 10^{-3}, 1.4 \times 10^{-3}, 7.2 \times 10^{-4}, 1.3 \times 10^{-4}, 4.5 \times 10^{-5}$ in (b), where we used the values of diffusion constant $D = 0.1, 0.05, 0.01, 0.005, 0.001, 0.0005$ and the Lamb-Dicke parameter $\eta = 0.25, 0.125, 0.0625, 0.03125$.

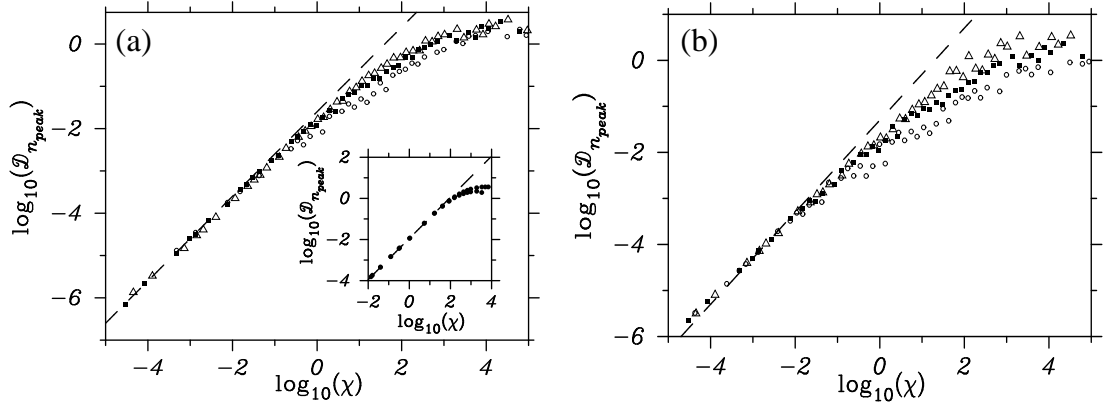


FIG. 7: The maximum distance between quantum and classical distributions given by the value of the first peak of \mathcal{D}_n at $n = n_{\text{peak}}$ as a function of χ . The initial distribution is centered at $\mathbf{x}_0 = (0, 1.1)$ in (a) and $\mathbf{x}_0 = (0.7, 0)$ in (b). The marks (\circ) are for $K = 0.5$, the (\blacksquare) for $K = 1.0$ and (\triangle) for $K = 1.5$. The region of linear behavior of $\mathcal{D}_{n_{\text{peak}}}$ as a function of χ is highlighted by the dashed line with unit value of the slope. The inset is the result borrow from [15] when the initial distribution explore a chaotic region in phase space of the classic KHO. We used the value of the Lamb-Dicke parameters $\eta = 0.5, 0.25, 0.125, 0.0625, 0.03125$ and the diffusion constant $D = 5 \times 10^{-6}, 1 \times 10^{-5}, 5 \times 10^{-5}, 1 \times 10^{-4}, 5 \times 10^{-4}, 1 \times 10^{-3}, 5 \times 10^{-3}, 1 \times 10^{-2}, 5 \times 10^{-2}, 10^{-1}$.

smoothed one

$$\tilde{L}(\mathbf{x}^R, \mathbf{x}') \equiv \int \frac{d\bar{\mathbf{x}}}{2\pi D} L(\bar{\mathbf{x}}, \mathbf{x}') \exp\left(-\frac{(\bar{\mathbf{x}} - \mathbf{x}^R)^2}{2D}\right), \quad (14)$$

here $D = \tilde{\Gamma}\tau$ is the diffusion constant between two consecutive kicks, and \mathbf{x}^R is the result of the harmonic evolution given in Eq.(7). Then, the classical smoothed propagator for the classical distribution function is

$$\tilde{L}^{cl}(\mathbf{x}^R, \mathbf{x}') = \frac{e^{-(x^2+y^2)}}{4\pi D}, \quad (15)$$

where $y = (p' - p^R + K \sin q') / 2\sqrt{D}$ and $x = (q' - q^R) / 2\sqrt{D}$. In the same way, we performed the integration in Eq.(14) over the the propagator in Eq.(6) to obtain the smoothed quantum propagator:

$$\tilde{L}(\mathbf{x}^R, \mathbf{x}') \equiv \int_{-\infty}^{+\infty} \frac{d\mu}{2\pi\eta^2} e^{-\frac{D\mu^2}{\eta^4}} e^{\frac{i}{\eta^2}[K \sin(q') \sin(\mu) - \mu(p^R - p')]} \delta(q^R - q'). \quad (16)$$

The presence of the Gaussian factor $\exp(-D\mu^2/\eta^4)$ in the integrand allows to obtain an approximation in terms of the classical smoothed propagator given in Eq.(15). Indeed, when the width of this Gaussian is small, $\eta^2/\sqrt{D} \ll 1$, the μ 's that effectively contribute to the integration are those close to the origin. So, it can be used $\sin(\mu) \approx \mu - \mu^3/6$ in the phase of the integrand. Moreover, if $\chi = K\eta^4/D^{3/2} \ll 1$, the term with μ^3 in the phase is small, so it also can be used $e^{i(\theta+\delta)} \approx e^{i\theta} + i\delta e^{i\theta}$ and then the μ -integration can be performed. Thus, it is obtained the following approximation to the smoothed quantum propagator:

$$\tilde{L}(\mathbf{x}^R, \mathbf{x}') \approx \tilde{L}^{cl}(\mathbf{x}^R, \mathbf{x}') [1 + \chi \sin(q') f(y)] , \quad (17)$$

where $f(y) = 1/4 (y - 2y^3/3)$. Since $|f(y) \exp(-y^2)| \leq 0.081$, Eq. (17) is valid under the less restrictive condition $\chi \lesssim 1$. It is important to note that the smoothed quantum propagator (Eq.(17)) is obtained without any assumption of the underlying classical dynamics of the system. The only conditions that have to be fulfilled are: **i)** $D \gg \eta^4$ and **ii)** $D \gtrsim (K\eta^4)^{2/3}$. These two conditions can be casted in $D \gtrsim (K\eta^4)^{2/3} \gg \eta^4$, which is always attainable in the semiclassical regime ($\eta \ll 1$), independently of the value of D .

The approximation of the quantum propagator [Eq.(17)] allows us to write the Wigner function immediately before the kick n as,

$$\tilde{W}_n(\mathbf{x}) = \tilde{W}_n^{cl}(\mathbf{x}) + \chi \sum_{j=0}^n \tilde{G}_j(\mathbf{x}) + \mathcal{O}(\chi^2) . \quad (18)$$

where the tilde indicates the action of the purely diffusive reservoir and we define the phase space function,

$$\begin{aligned} \tilde{G}_j(\mathbf{x}) &= \int d\mathbf{x}_n \tilde{L}^{cl}(\mathbf{x}^R, \mathbf{x}_n) \\ &\vdots \\ &\times \int d\mathbf{x}_j \sin(q_j) f(y_j) \tilde{L}^{cl}(\mathbf{x}_j^R, \mathbf{x}_{j-1}) \times \\ &\vdots \\ &\times \int d\mathbf{x}_0 \tilde{L}^{cl}(\mathbf{x}_1^R, \mathbf{x}_0) W_0(\mathbf{x}_0) . \end{aligned} \quad (19)$$

Eq.(18) is obtained iterating the evolution given by Eq.(5) with the smoothed Wigner propagator in Eq.(17) from the initial condition $W_0(\mathbf{x}_0)$, and keeping only terms of first order in χ . Hence, when $\chi \ll 1$ we get for the separation between the classical and quantum distributions,

$$\mathcal{D}_n \approx \chi \int d\mathbf{x} \left| \sum_{j=0}^n \tilde{G}_j(\mathbf{x}) \right| . \quad (20)$$

The scaling law proportional to χ is confirmed in Fig. 6 where we displayed \mathcal{D}_n/χ as a function of the number of

kicks n for $K = 0.5$ and $K = 1.5$ and a wide range of values of η and D . We can see that for order of magnitude different values of χ , all the curves \mathcal{D}_n/χ .vs. n fit in the same scale. So, independently of the value of D , in the semiclassical limit we have $D \gg (K\eta^4)^{2/3} \gg \eta^4$, and thus the separation between the quantum and the classical distributions goes down with η^4 , becoming arbitrarily small. The curves in Fig. 6 were generated for an initial coherent state whose Gaussian Wigner function, $W_0(\mathbf{x}_0)$, is centered in the phase space point $\mathbf{x}_0 = (0, 1.1)$ (Fig. 1) but we get similar results when $W_0(\mathbf{x}_0)$ is centered at $\mathbf{x}_0 = (0.7, 0)$. It is worth to remember that the initial distributions considered explore regions of phase space with essentially regular classical dynamics when $K=0.5$, while for $K=1.5$ these regions correspond to a mixed classical dynamics. We have also obtained similar results when we considered the case with $K = 1$.

The range of values of χ for which the approximation in Eq.(20) works is showed in Fig. 7 where we plot the first peak of \mathcal{D}_n , that corresponds to the maximum separation between the classical and the quantum distributions, as a function of χ . We can see that the proportionality of \mathcal{D}_n with χ is in general valid for $\chi < 1$ with a slightly dependence with the position in phase space of the initial distribution. We also observe that, when the phase space regions explored by the initial distribution are regular or mixed the proportionality is valid up to values $\mathcal{D}_n < 1$ while if the regions explored are essentially chaotic the proportionality with χ is valid up to $\mathcal{D}_n \approx 1$ (see inset of Fig. 7).

It is interesting to compare the behavior of the time position of the first peak of \mathcal{D}_n as a function of η of our curves with its behavior when $K = 2$ found in [15]. In that case the initial distribution was centered at the origin of phase space, that for $K = 2$ it is an hyperbolic fixed point surrounded by a chaotic region (Fig. 1(d)). The time position of the peak occurred approximately for $n_{\text{peak}}(\eta) \approx (1/\Lambda) \ln(1/\eta)$ where Λ is the expansion eigenvalue of the linear map at the origin. However, in our case the time position of the first peak of \mathcal{D}_n is almost the same for all values of η . Note that the first peak of \mathcal{D}_n points the moment when the decoherence effects start to dominate, restraining the tendency to the separation of the classical and quantum distributions produced by the presence of nonlinearities in the system. When the underlying classical dynamics is chaotic these nonlinearities are reached in a very short time, so the diffusion dominates when these nonlinearities have already been reached. This reflects in the behavior of the position of the peak that it is a memory of the behavior of the separation time Eq.(10) without the action of a reservoir, although lost its meaning due to the smallness of \mathcal{D}_n . On the contrary, when the underlying classical dynamics is regular or mixed the time to reach the nonlinearities is very slow so almost immediately the diffusion washed out any memory, in the position of peak, of the separation time in Eq.(11).

Our numerical simulations together with those in [15]

show that the scale-law in Eq.(20) rules the quantum to classical transition of the KHO in the semiclassical regime and in the presence of decoherence, independently of the underlying classical behavior. This is a consequence of the approximation in Eq.(18). Therefore, the same scale-law proportional to χ is valid for the mean values of any smooth observables throughout the evolution of the system. Indeed, the mean value of an observable \hat{O} in a state represented by the Wigner function $W(\mathbf{x})$ is given by

$$\langle \hat{O} \rangle = \int d\mathbf{x} O(\mathbf{x}) W(\mathbf{x}) \quad , \quad (21)$$

where $O(\mathbf{x})$ is the Weyl symbol of \hat{O} obtained through the Weyl transform in Eq.(4) replacing $\hat{\rho}/4\pi\eta^2 \rightarrow \hat{O}$ [3]. The classical mean value is obtained in the same way substituting $O(\mathbf{x})$ by the classical function $O^{cl}(\mathbf{x})$ and $W(\mathbf{x})$ by the classical distribution $W^{cl}(\mathbf{x})$. So, for every smooth operator in the semiclassical regime we can take $O(\mathbf{x}) \approx O^{cl}(\mathbf{x})$ [27] and in the presence of decoherence we use the result in Eq.(18) to get

$$\langle \hat{O} \rangle_n - \langle \hat{O} \rangle_n^{cl} = \chi \int d\mathbf{x} O_n^{cl}(\mathbf{x}) \sum_{j=0}^n \tilde{G}_j(\mathbf{x}) + \mathcal{O}(\chi^2) \quad . \quad (22)$$

V. FINAL REMARKS

We study the effect of decoherence in the quantum-classical transition of the KHO when the classical dynamics is regular or mixed (with small regions of chaotic behavior). Our approach is based on the behavior of the distance \mathcal{D}_n [Eq.(12)] as a function of time. We show that without the presence of a reservoir, \mathcal{D}_n clearly indicates that the quantum unitary evolution separates from the classical evolution because it reaches values that do not decrease in the classical limit. When the initial distribution explore regions of regular classical dynamics, the separation time t_s scales as a potential law with the effective Planck constant, that is, $t_s \approx \tau/\hbar_{\text{eff}}^\alpha$. We observe

that when the degree of mixing increase this potential-law is not valid anymore.

When the system is in contact with a purely diffusive reservoir, we extend the results of Ref. [15] for regular and mixed classical dynamics, showing that in these regimes \mathcal{D}_n is also proportional to $\chi = K\hbar_{\text{eff}}^2/4D^{3/2}$ when $\chi < 1$. This implies that, in the semiclassical regime ($\hbar_{\text{eff}} \ll 1$), and independently of the values of the diffusion constant D and the classical dynamics explored by the initial distribution, the quantum-classical differences \mathcal{D}_n goes to zero as \hbar_{eff}^2 . The conditions for the proportionality between \mathcal{D}_n and χ can be condensed in the inequality $D \gg (K\hbar_{\text{eff}}^2)^{2/3} \gg \hbar_{\text{eff}}^2$ that is the relation of the strength of noise and the semiclassical parameter for the KHO in order to obtain correctly the classical limit for all the regimes of its underlying classical dynamics. Finally, we can say that because of the smallness of \mathcal{D}_n , in the semiclassical regime, the concept of separation time is not meaningful anymore.

Although in the framework of an specific model, our results and those in Ref. [15], indicates that the conjecture presented in Ref. [16], that in the presence of noise a single parameter χ controls the quantum-classical transition of classically chaotic systems, may be extended in general for all type of classical dynamics. However, it seems that in χ should enters only a parameter that controls the degree of mixing of the considered system and not directly the Lyapunov coefficient that characterize the exponential divergence of trajectories in fully chaotic classical systems.

VI. ACKNOWLEDGMENTS

We acknowledge Luiz Davidovich for fruitful comments. DAW gratefully acknowledges support from CONICET(Argentina) and PROSUL(Brazil). FT acknowledges the hospitality at the "Departamento de Física "J. J. Giambiagi"", FCEN, UBA, where this work started.

-
- [1] L. E. Ballentine, Yumin Yang, and J. P. Zibin , Phys. Rev. A **50**, 2854 (1994).
 - [2] E. Wigner, Phys. Rev. **40**, 749 (1932).
 - [3] M. Hillery, R. F. O'Connell, M. O. Scully and E. P. Wigner, Phys. Rep. **106**, 121 (1984).
 - [4] G. P. Berman and G. M. Zaslavsky, Physica A **91**, 450 (1978).
 - [5] M. V. Berry, N. L. Balazs, M. Tabor and A. Voros, Ann. Phys. **122**, 26 (1979).
 - [6] B.V. Chirikov, F. M. Izrailev and D. L. Shepelyansky, Physica D **33** 77 (1988).
 - [7] G. P. Berman, V. Yu Rubaev and G. M. Zaslavsky, Non-linearity **4**, 543 (1991).
 - [8] Z. P. Karkuszewski, J. Zakrzewski, and W. H. Zurek, Phys. Rev. A **65**, 042113 (2002).
 - [9] A. R. R. Carvalho, R. L. de Matos Filho and L. Davidovich, Phys. Rev. E **70**, 026211 (2004).
 - [10] L. Davidovich, F. Toscano, and R. L. de Matos Filho, *Decoherence and the Quantum-Classical Transition in Phase Space in AIP Conference Proceedings, ATOMIC PHYSICS 19: XIX International Conference on Atomic Physics-ICAP 2004*, Editors: L. G. Marcassa, K. Helmersson, V. S. Bagnato, May 5, 2005, Volume 770, Issue 1, pp. 301-310. L. Davidovich, F. Toscano, and R. L. de Matos Filho; *Decoherence and the quantum-classical limit in phase space in Proceedings of SPIE -The International*

- Society for Optical Engineering, Volume 5842, "Fluctuations and Noise in Photonics and Quantum Optics III",* Editors: P. R. Hemmer, J. R. Gea-Banacloche, P. Heszler, Sr., M. S. Zubairy, May 2005, pp. 220-231.
- [11] W. H. Zurek and J. P. Paz, in *Numerical exploration of Hamiltonian systems*, Proceedings of Les Houches (1981), session XXXVI (North Holland, 1983), section 7, p. 136. W. H. Zurek, Phys. Scr., **T76**, 186 (1998). M. Berry, in *Quantum mechanics: Scientific perspectives on Divine Action*, edited by K. W.-M. R. J. Russell, P. Clayton and J. Polkinghorne (Vatican Observatory - CTNS Publications, 2001), pp. 4154.
 - [12] W. H. Zurek and J. P. Paz, Phys. Rev. Lett. **72** 2508 (1994).
 - [13] W. H. Zurek, Rev of Mod. Phys., **75**, 715 (2003).
 - [14] I. Garcia-Mata and M. Saraceno, Mod. Phys. Lett. B **19**, 341 (2005)
 - [15] F. Toscano, R. L. de Matos Filho and L. Davidovich, Phys. Rev. A **71**, 010101(R) (2005).
 - [16] A. K. Pattanayak, B. Sundaram and Benjamin D. Greenbaum, Phys. Rev. Lett. **90** 014103 (2003).
 - [17] S. A. Gardiner, J. I. Cirac, and P. Zoller, Phys. Rev. Lett. **79**, 4790, (1997).
 - [18] D. J. Wineland, C. Monroe, W. M. Itano, D. Leibfried, B. E. King and D. M. Meekhof, Journal of Research of the National Institute of Standards and Technology **103**, 259 (1998).
 - [19] J. Bertrand and P. Bertrand: Found. Phys. **17**, 397 (1987).
 - [20] L. G. Lutterbach and L. Davidovich, Phys. Rev. Lett. **78**, 2547 (1997); P. Bertet, A. Auffeves, P. Maioli, S. Osnaghi, T. Meunier, M. Brune, J. M. Raimond, and S. Haroche, Phys. Rev. Lett. **89**, 200402 (2002); F. de Melo, L. Aolita, F. Toscano and L. Davidovich, Physical Review A **73**, 030303 (2006).
 - [21] H. J. Korsch and M. V. Berry, Physica 3D, 627 (1981).
 - [22] R. L. Hudson, Rep. Math Phys. **6**, 249 (1974).
 - [23] J. E. Moyal, Proc. Cambridge Phils. Soc. **45**, 99 (1949).
 - [24] D. Monteoliva and J. P. Paz, Phys. Rev. E, **64**, 056238 (2001).
 - [25] M. Henon, "Numerical exploration of Hamiltonian systems", Proceedings of Les Houches (1981), session XXXVI (North Holland, 1983), section 7, p. 136.
 - [26] For each value of η , the quantity \mathcal{D}_n saturate at a different value always larger than one (not showed in the graph (a) in Fig. 2).
 - [27] A. M. Ozorio de Almeida, Phys. Rep. **295**, 265 (1998).